Lagged relationships between ENSO and the Asian Summer Monsoon in the CSIRO coupled model

Ryuichi Kawamura
Department of Earth Sciences, Toyama University, Toyama, Japan

Ramasamy Suppiah, Mark A. Collier, and Hal B. Gordon
Division of Atmospheric Research, CSIRO, Aspendale, Victoria, Australia

Received 2 September 2004; revised 11 October 2004; accepted 9 November 2004; published 10 December 2004.

[1] The lagged relationship between the El Nino-Southern Oscillation (ENSO) and Asian Summer Monsoon (ASM) variability is investigated using the Commonwealth Scientific and Industrial Research Organization (CSIRO) Mark3 coupled model. Composite analyses of 17 warm and 16 cold events from an extended unforced run reveal that the model captures the asymmetric structures of rainfall and SST anomalies over the tropical Indian Ocean during northern hemisphere spring which is one of the major precursory signals of anomalous ASM variability. As a remote forcing mechanism prior to the ASM onset, simulated anomalous convection over the northern Indian Ocean strongly influences the land surface hydrologic conditions over central and southwest Asia. Simulated land-surface processes result in anomalous temperatures over the land, which in turn produce a change in the land-ocean thermal contrast over the domain. The results are consistent with observed features, which show a delayed and indirect impact of ENSO on the ASM variability during the early summer monsoon period, but not during the rest of the monsoon season. *INDEX TERMS:* 1620 Global Change: Climate dynamics (3309); 3339 Meteorology and Atmospheric Dynamics: Ocean/atmosphere interactions (0312, 4504); 3374 Meteorology and Atmospheric Dynamics: Tropical meteorology; 3319 Meteorology and Atmospheric Dynamics: General circulation; 3309 Meteorology and Atmospheric Dynamics: Climatology (1620). **Citation:** Kawamura, R., R. Suppiah, M. A. Collier, and H. B. Gordon (2004), Lagged relationships between ENSO and the Asian Summer Monsoon in the CSIRO coupled model, *Geophys. Res. Lett.*, *31*, L23205, doi:10.1029/2004GL021411.

1. Introduction

[2] The Asian-Australian monsoon is the largest atmospheric circulation system in the world, straddling two continents (the Asian and Australian continents) and two ocean basins (the Indian and Pacific Oceans). Previous studies have demonstrated a strong relationship between the Asian-Australian summer monsoon system and the El Nino-Southern Oscillation (ENSO) phenomenon [e.g., *Shukla and Paolino*, 1983; *Rasmusson and Carpenter*, 1983; *Holland*, 1986; *Meehl*, 1987; *Webster and Yang*, 1992; *Suppiah*, 1992]. Due to the location of the Australian continent, the interannual variability of the Australian monsoon is strongly influenced by the peak phase of ENSO through the anomalous Walker circulation over the tropical Pacific Ocean during the southern hemisphere summer. However, the link between the Indian summer monsoon, which lasts from May to September, and ENSO is strongest during the development and decay stages of the ENSO phenomenon. It is thus interesting that, despite such unfavorable conditions (locations and season) during the Indian monsoon, the relationship between the Asian Summer Monsoon (ASM) and ENSO is very robust. Therefore, an investigation of the ASM-ENSO relationship during both the development and the decay phases of ENSO is warranted.

[3] The direct impact of ENSO on the monsoon system during its growth phase has been investigated by *Lau and Wu* [2001], and *Kawamura et al.* [2003]. *Lau and Wu* [2001] demonstrated a link between ENSO and ASM using the first singular value decomposition (SVD) mode, which was derived from tropical rainfall and sea surface temperature (SST) anomalies over the tropical Indian and Pacific Oceans. In a subsequent study, *Kawamura et al.* [2003] suggested that this sort of ENSO-ASM link might have dominated during the period from the 1960s to mid-1970s when biennial oscillation (BO)-like ENSO was prominent, because the ASM season often corresponds to the development phase of the BO-like ENSO. A number of studies considered the BO-like feature of ENSO as an oscillation independent of ENSO, which is named as the Tropospheric Biennial Oscillation (TBO), and discussed the TBO-ASM links [e.g., *Meehl*, 1997; *Chang and Li*, 2000; *Kim and Lau*, 2001; *Meehl and Arblaster*, 2002; *Yu et al.*, 2003].

[4] Since the late 1970s, severe and extended El Niños with a 4–5 year periodicity have tended to dominate the ENSO cycle [e.g., *Mitchell and Wallace*, 1996; *Torrence and Webster*, 1999]. A change in the ENSO cycle after the late 1970s has resulted in a change in the relationship between ENSO and ASM during its mature phase [*Yang et al.*, 1996; *Yang and Lau*, 1998; *Kawamura et al.*, 2001]. Moreover, *Yang et al.* [1996] and *Yang and Lau* [1998] revealed that ENSO in the preceding winter and spring have an indirect link with the ASM through land-surface hydrologic processes over the Asian continent. In subsequent observational studies [*Kawamura*, 1998; *Kawamura et al.*, 2001], a stronger than average upper-level circulation west of the Tibetan Plateau was noticed during the preceding spring as a result of a dynamic response to increased convection over the northern Indian Ocean and the maritime continent. The changes in convection affect land-surface

0094-8276/04/2004GL021411$05.00

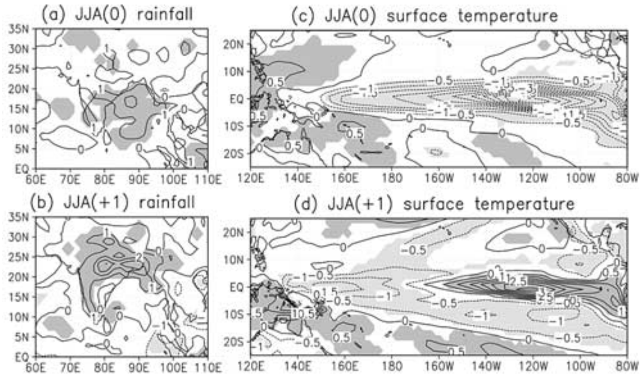

Figure 1. Differences between composites of surface temperature and rainfall anomalies from cold and warm events for JJA (year 0) and JJA (year +1). The "year 0" and "year +1" denote reference and subsequent years, respectively. Contour intervals for rainfall and temperature are 1 mm day^{-1} and 0.5°C, respectively. Shading indicates the regions where values are different from zero at the 5% level of statistical significance using a Student's *t*-test.

hydrologic conditions and hence the characteristics of synoptic-scale disturbances over central and southwest Asia. The above-mentioned dynamic process was confirmed from observational records and by the numerical experiments of *Barlow et al.* [2002] who investigated the causes of severe droughts that affected central and southwest Asia for three consecutive years.

[5] The ENSO characteristics of coupled ocean-atmosphere models (CGCMs) have been documented in a variety of ways in the literature [e.g., *Philander et al.*, 1992; *Meehl et al.*, 2001; *Cordon et al.*, 2001]. However, few CGCMs have been shown to simulate the delayed and indirect impact of ENSO on the ASM so far. In this study, we use the results from the CSIRO Mark3 CGCM to see whether this model can reproduce some of the observed characteristics of lagged relationships between ENSO and the ASM, and also some of the dynamic features associated with increased convective activity over the Indian Ocean.

2. Data Used and Analysis Procedure

[6] The atmospheric component of the CSIRO Mark3 coupled model has a horizontal resolution of T63 (approximately 1.875° longitude by 1.875° latitude) and 18 vertical levels. A detailed description of the physical processes is given by *Gordon et al.* [2002]. The oceanic component of the coupled model is based on the Modular Ocean Model version 2.2 (MOM2.2) of the Geophysical Fluid Dynamics Laboratory [*Pacanowski*, 1996]. The ocean model has a horizontal resolution of 1.875° longitude by 0.9375° latitude. The horizontal resolution of the ocean model matches the atmospheric model grid in the zonal direction, but twice that in the meridional direction. The ocean has 31 vertical levels, of which 14 levels represent the upper 400 m.

[7] Simulated data from model years 201 to 300 of a multi-century control simulation have been used in this analysis, as the model simulated global mean surface temperature showed a small climate drift before year 200, and little thereafter [*Gordon et al.*, 2002]. Compared to observations, the model simulated amplitude of the Nino3-SST index is larger in boreal summer than in winter and also shows a pronounced 2–3 year periodicity. On the basis of the Nino3-SST index for June-to-August (JJA), we have selected 17 warm events and 16 cold events that exceed one standard deviation. Composite maps were then constructed for surface temperature, rainfall, wind stress, and stream function.

3. Results

[8] Figure 1 shows differences in rainfall anomalies for the ASM region and surface temperature anomalies for the Pacific Ocean between cold and warm events for JJA (year 0) and JJA (year +1). Here the "year 0" and "year +1" denote the current year and the subsequent year of the mature ENSO phase, respectively. In JJA (0), negative SST anomalies are zonally elongated over the equatorial Pacific, while positive rainfall anomalies are simulated over the Indian subcontinent and the Bay of Bengal, implying a stronger summer monsoon. This anomalous feature results from the direct ENSO influence on ASM during its growth phase as a result of an intense Walker circulation over the tropical Pacific and Indian Oceans [e.g., *Lau and Wu*, 2001; *Kawamura et al.*, 2003]. The cold event of ENSO terminates in the early months of the subsequent year, but a warm event tends to develop over the eastern equatorial Pacific in JJA (+1). The development of a warm event usually leads to a weak relationship with ASM in JJA. However, positive rainfall anomalies that cover the Indian subcontinent during JJA (+1) reveal a stronger monsoon despite the occurrence of the warm event in the model simulation.

[9] Figure 2 displays the lag-relationship between Indian and Australian rainfall anomalies and SST anomalies over Pacific and Indian Oceans. The strength of the monsoon activity is given here as the difference in cold and warm events' rainfall anomalies averaged over the region (70°–90°E, 10°–25°N) for the Indian monsoon and over the region (115°–155°E, 10°–25°S) for the Australian monsoon (AM). Simulated Nino-3 and Nino-3.4 SST anomalies represent modeled ENSO variability, together with the Indian Ocean SST anomalies averaged over the region (50°–100°E, 10°S–10°N). Note that the reference month is July (0). When cold events develop in boreal summer, the ASM rainfall tends to be above average from May (0) to

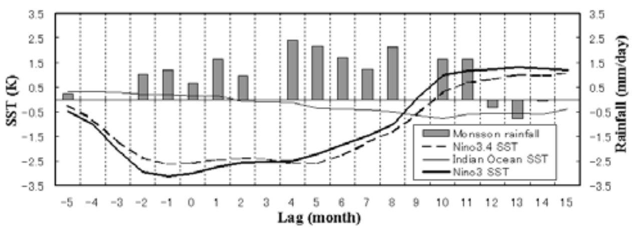

Figure 2. Lag-relationship between simulated ENSO and monsoon rainfall. Bars depict composite monsoon rainfall, while lines show SST anomalies. For example, the "lag 0", "lag 6", and "lag 12" denote July (year 0), January (year +1), and July (year +1), respectively. The monsoon rainfall anomalies refer to ASM (May–September) and AM (November–March).

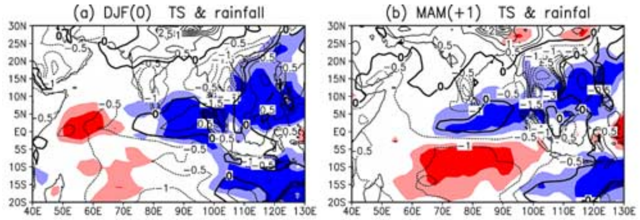

Figure 3. Difference between composites of surface temperature and rainfall anomalies from cold and warm events (former minus latter) for DJF (year 0) and MAM (year +1). Contour interval for temperature is 0.5°C. Significant positive and negative rainfall anomalies are denoted by blue and red colors, respectively.

September (0). As in the observed records, the persistence of cold events leads to increased rainfall over AM region from November (0) to March (+1). A strong Asian summer monsoon is followed by a strong Australian summer monsoon [e.g., *Meehl*, 1997; *Chang and Li*, 2000].

[10] Cold events tend to decay from early the following year (January (+1)) and terminate by boreal spring. Subsequently, warm events develop around May (+1) and persist until the following summer. The sign of the tropical Indian Ocean SST anomalies changes from positive to negative in autumn, and the negative anomalies are further strengthened until early into the next summer. As a result, the east-west gradient of SST anomalies between the tropical Pacific and Indian Oceans is reversed around May (+1). These SST evolutions are comparable to those reported for the TBO [*Meehl and Arblaster*, 2002; *Yu et al.*, 2003]. Another significant feature is the above normal rainfall over ASM region in May and June, despite the development of the warm event and below normal rainfall at the late stage of monsoon season. Figure 1b also shows that the strong ASM results in above-normal rainfall at the early stage of the subsequent monsoon season.

[11] To examine whether there are any precursory signals for the anomalous ASM in the subsequent summer, we have calculated differences between composites of surface temperature and rainfall anomalies over the tropical Indian Ocean for cold and warm events for DJF (year 0) and MAM (year +1). Results are shown in Figure 3. In DJF (year 0), positive rainfall anomalies dominate from the South China Sea to the eastern half of equatorial Indian Ocean, corresponding closely to the area of positive SST anomalies. In contrast, negative rainfall and SST anomalies dominate (occupy) the western half of the tropical Indian Ocean. However, such a zonally asymmetric structure of rainfall anomalies disappears in MAM. Rather, an equatorially asymmetric structure of anomalous rainfall is established in conjunction with a similar structure of SST anomalies. Positive (negative) rainfall anomalies are evident to the north (south) of the equator. Significant changes, which occur as precursory signals of the anomalous ASM during the transitional season in the CSIRO simulation, are very similar to observed conditions, particularly after the late 1970s [e.g., *Ju and Slingo*, 1995; *Kawamura*, 1998]. *Kawamura et al.* [2001] found agreement with the positive wind-evaporation-SST (WES) feedback proposed by *Xie and Philander* [1994] which is critical for the generation and maintenance of the equatorial asymmetries over the tropical Indian Ocean in spring.

[12] Figures 4a–4d show differences between cold and warm composites for 200-hPa stream function, rainfall, soil moisture, short-wave radiation, and land surface temperature anomalies for MAM (year +1). As previously mentioned, enhanced convection indicated by increased rainfall is evident over the northern tropical Indian Ocean. As a result of a dynamic response to enhanced off-equatorial convection, a stronger anticyclonic circulation is formed in the upper troposphere over central and southwest Asia, including the Tibetan Plateau. Due to this dynamic process, central and southwest Asia, including the Tibetan Plateau show decreased rainfall, and often experience severe droughts as reported by, e.g., *Barlow et al.* [2002], from observed records. As a result of enhanced anticyclonic circulation leading to clear-sky conditions, incoming short-wave radiation increases over central and southwest Asia (Figure 4c). Furthermore, the decrease in soil moisture closely coincides with that of the rainfall decrease, except for part of the Tibetan Plateau. The combined effect of decreased soil moisture and increased incoming short-wave radiation results in land-surface warming during the pre-monsoon season (see Figure 4d). Moreover, these processes suggest that the increased convection over the northern Indian Ocean act as a remote forcing that substantially influences land surface hydrologic conditions over central and southwest Asia. Furthermore, the anomalously land-surface warming enhances the land-sea thermal contrast prior to monsoon onset, which eventually serves as a significant factor for a stronger ASM. The reverse processes occur during a weak ASM. It is evident from the results presented here that the model simulates the indirect impact of ENSO on the ASM through land-surface hydrologic processes during its decay phase, as has been suggested

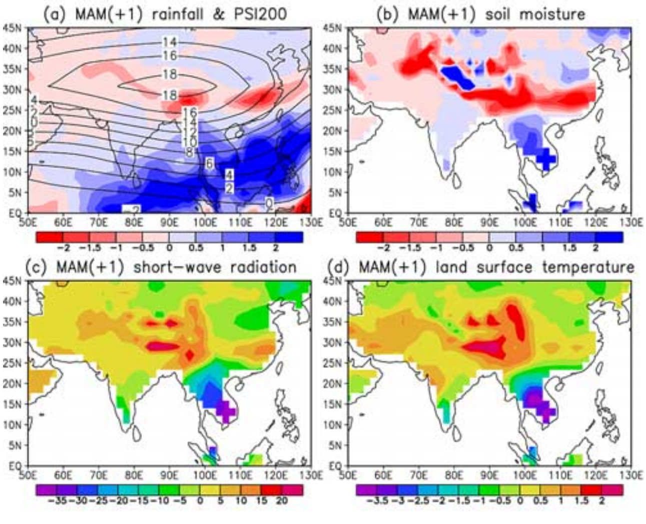

Figure 4. Difference between the composites of (a) 200-hPa stream function and rainfall, (b) soil moisture, (c) short-wave radiation, and (d) land surface temperature anomalies from cold and warm events (former minus latter) for MAM (year +1). Contour interval for stream function is 2×10^5 m^2 s^{-1}.

by *Kawamura* [1998] and *Kawamura et al.* [2001]. This delayed impact (lagged relationship) is consistent with the findings from observational records. The indirect ENSO impact plays a significant role in affecting the ASM variability in early summer, but does not persist until late summer (see Figure 2).

[13] As mentioned in the introduction, the indirect ENSO impact through the land-surface hydrologic processes is expected to dominate the ENSO-ASM link when the ENSO has longer periodicity. One may wonder why the CSIRO coupled model is successful in simulating the indirect impact of ENSO on the ASM despite the model ENSO having a 2–3 year periodicity. One possible explanation is that positive SST anomalies over the eastern tropical Indian Ocean, the South China Sea and the Philippine Sea persist from DJF (0) to MAM (+1) as seen in Figure 3, which is significantly different from the features reported for the TBO. The positive SST anomalies lead to enhanced convection and may thus be responsible for the generation of the equatorial asymmetries over the tropical Indian Ocean in MAM of the following year.

4. Summary

[14] We have analyzed an extended unforced run of the CSIRO Mark3 Coupled Ocean GCM to investigate the characteristics of the observed delayed impact (lagged relationship) between ENSO and the Asian Summer Monsoon (ASM). Composite analysis of 17 warm events and 16 cold events shows that the model captures features of the equatorially asymmetric structures of rainfall and SST anomalies observed over the tropical Indian Ocean during the pre-monsoon season, which is one of the major precursory signals of an anomalous ASM. The model also simulates a stronger upper-tropospheric anticyclonic circulation over central and southwest Asia induced by a dynamic response to strong convective activity over the northern Indian Ocean. These circulation anomalies lead to a strong land-sea temperature gradient prior to the monsoon onset through hydrologic processes. It is also demonstrated that a delayed and indirect ENSO impact plays a significant role in influencing the ASM variability especially in early summer.

[15] This study emphasizes the importance of the lagged impacts of ENSO on the ASM which in turn indicates the basis for a robust link between ENSO and the ASM. Since the CSIRO Mark3 CGCM model captures the observed link between ENSO and ASM under present climate conditions, we intend to investigate the presence of a link between ENSO and ASM, under enhanced greenhouse conditions. These results will be reported in a subsequent paper.

[16] **Acknowledgments.** This research was supported by the research project "R&D of hydrological modeling and water resources system" of JST/CREST, and by the research project "Refinement of global and regional water cycle", and Grants-in-Aids (14540406) of the Japanese Ministry of Education, Sports, Culture, Science and Technology. The model development at CSIRO Atmospheric Research is supported by the Australian Greenhouse Office and funds from States and Territories.

References

Barlow, M., H. Cullen, and L. Bradfield (2002), Drought in central and southwest Asia: La Nina, the warm pool, and Indian Ocean precipitation, *J. Clim.*, *15*, 697–700.

Chang, C.-P., and T. Li (2000), A theory for the tropical tropospheric biennial oscillation, *J. Atmos. Sci.*, *57*, 641–651.

Cordon, F., A. Vintzlieos, and R. Sadourny (2001), Influence of mean state changes on the structure of ENSO in a tropical coupled GCM, *J. Clim.*, *14*, 730–742.

Gordon, H. B., et al. (2002), The CSIRO Mk3 climate system model, *Tech. Pap.60*, 130 pp., CSIRO Division of Atmospheric Research, Aspendale, Australia.

Holland, G. J. (1986), Interannual variability of the Australian summer monsoon at Darwin: 1952–82, *Mon. Weather Rev.*, *114*, 594–604.

Ju, J., and J. M. Slingo (1995), The Asian summer monsoon and ENSO, *Q. J. R. Meteorol. Soc.*, *121*, 1133–1168.

Kawamura, R. (1998), A possible mechanism of the Asian summer monsoon–ENSO coupling, *J. Meteorol. Soc. Jpn.*, *76*, 1009–1027.

Kawamura, R., T. Matsuura, and S. Iizuka (2001), Role of equatorially asymmetric sea surface temperature anomalies in the Indian Ocean in the Asian summer monsoon and El Nino–Southern Oscillation coupling, *J. Geophys. Res.*, *106*, 4681–4693.

Kawamura, R., T. Matsuura, and S. Iizuka (2003), Equatorially symmetric impact of El Nino–Southern Oscillation on the South Asian summer monsoon system, *J. Meteorol. Soc. Jpn.*, *81*, 1329–1352.

Kim, K.-M., and K.-M. Lau (2001), Dynamics of monsoon-induced biennial variability in ENSO, *Geophys. Res. Lett.*, *28*, 315–318.

Lau, K.-M., and H. T. Wu (2001), Principal modes of rainfall-SST variability of the Asian summer monsoon: A reassessment of the monsoon-ENSO relationship, *J. Clim.*, *14*, 2880–2895.

Meehl, G. A. (1987), The annual cycle and interannual variability in the tropical Pacific and Indian Ocean regions, *Mon. Weather Rev.*, *115*, 27–50.

Meehl, G. A. (1997), The South Asian monsoon and the tropospheric biennial oscillation, *J. Clim.*, *10*, 1921–1943.

Meehl, G. A., and J. M. Arblaster (2002), The tropospheric biennial oscillation and Asian-Australian monsoon rainfall, *J. Clim.*, *15*, 722–744.

Meehl, G. A., P. R. Gent, J. M. Arblaster, B. L. Otto-Bliensner, E. C. Brady, and A. Craig (2001), Factors that affect the amplitude of El Nino in global coupled climate models, *Clim. Dyn.*, *17*, 515–526.

Mitchell, T. P., and J. M. Wallace (1996), ENSO seasonality: 1950–78 versus 1979–92, *J. Clim.*, *9*, 3149–3161.

Pacanowski, R. C. (1996), Documentation user's guide and reference manual (MOM2, Version 2), *GFDL Ocean Tech. Rep. 3.2*, 329 pp., Geophys. Fluid Dyn. Lab., Princeton, N. J.

Philander, S. G. H., N. C. Lau, R. C. Pacanowski, and M. J. Nath (1992), Simulation of ENSO with a global atmospheric GCM coupled to a high-resolution, tropical Pacific Ocean GCM, *J. Clim.*, *5*, 308–329.

Rasmusson, E. M., and T. H. Carpenter (1983), The relationship between eastern equatorial Pacific sea surface temperatures and rainfall over India and Sri Lanka, *Mon. Weather Rev.*, *111*, 517–528.

Shukla, J., and D. A. Paolino (1983), The Southern Oscillation and long-range forecasting of the summer monsoon rainfall over India, *Mon. Weather Rev.*, *111*, 1830–1837.

Suppiah, R. (1992), The Australian summer monsoon: A review, *Prog. Phys. Geogr.*, *16*, 283–318.

Torrence, C., and P. J. Webster (1999), Interdecadal changes in the ENSO-monsoon system, *J. Clim.*, *12*, 2679–2690.

Webster, P. J., and S. Yang (1992), Monsoon and ENSO: Selectively interactive systems, *Q. J. R. Meteorol. Soc.*, *118*, 877–926.

Xie, S.-P., and S. G. H. Philander (1994), A coupled ocean-atmosphere model of relevance to the ITCZ in the eastern Pacific, *Tellus*, *46A*, 340–350.

Yang, S., and K.-M. Lau (1998), Influences of sea surface temperature and ground wetness on Asian summer monsoon, *J. Clim.*, *11*, 3230–3246.

Yang, S., K.-M. Lau, and M. Sankar-Rao (1996), Precursory signals associated with the interannual variability of the Asian summer monsoon, *J. Clim.*, *9*, 949–964.

Yu, J.-Y., S.-P. Weng, and J. D. Farrara (2003), Ocean roles in the TBO transitions of the Indian-Australian monsoon system, *J. Clim.*, *16*, 3072–3080.

M. A. Collier, H. B. Gordon, and R. Suppiah, Division of Atmospheric Research, CSIRO, 107-121 Station Street, Aspendale, Victoria 3195, Australia.

R. Kawamura, Department of Earth Sciences, Toyama University, 3190 Gofuku, Toyama 930-8555, Japan. (kawamura@sci.toyama-u.ac.jp)